Photoreactive Zn(II) Coordination Compounds: Exploring Biomimetic Mechanical Motion and Photosalient Behavior

Uma Kurakula,[a,‡] Akansha Ekka,[a,‡] Basudeb Dutta,[c] Mohammad Hedayetullah Mir,[c] Nathan R. Halcovitch,[b] and Raghavender Medishetty*[a]*

a. Department of Chemistry, Indian Institute of Technology Bhilai, Kutelabhata, Durg, 491001, Chhattisgarh, India. raghavender@iitbhilai.ac.in; ragha.chem@gmail.com

b. Chemistry Department, Lancaster University, Faraday Building, Lancaster University, Lancaster, LA1 4YB, UK.

c. Department of Chemistry, Aliah University, New Town, Kolkata 700160, India. chmmir@gmail.com

‡ These authors contributed equally.

KEYWORDS. [2+2] photoreaction, isostructural complexes, photosalient effect, jumping crystals, peeling crystals, photoluminescence.

ABSTRACT: Locomotion plays a pivotal role in the survival of most organisms, enabling essential activities such as foraging, predator evasion, and reproduction. In the realm of biomimetics, seed pod explosion, bark peeling – a well-established biological mechanism employed by various plant species for defense and reproduction – offers a fascinating avenue for exploration. In this study, we present six novel photoreactive Zn(II)-based coordination compounds capable of significant mechanical motion, including explosion and peeling effect under UV light irradiation. These compounds were synthesized using aryl derivatives of 4-vinylpyridines, namely 4spy (4-styrylpyridine), 3tpy (4-(3-(thiophene-3-yl)vinyl)pyridine), and 2tpy (4-(2-(thiophene-2-yl)vinyl)pyridine), in conjunction with chloride or bromide co-linkers. The resulting complexes, $[ZnCl_2(4spy)_2]$ (**1**), $[ZnCl_2(3tpy)_2]$ (**2**), $[ZnCl_2(2tpy)_2]$ (**3**), $[ZnBr_2(4spy)_2]$ (**4**), $[ZnBr_2(3tpy)_2]$ (**5**), and $[ZnBr_2(2tpy)_2]$ (**6**), were characterized as isostructural, with slight variations observed in compound **6**'s structural packing. X-ray diffraction analysis confirmed the tetrahedral geometry of Zn(II) in all the six complexes. Notably, compounds **1**-**5** exhibited coordination involving both planar and non-planar linkers, leading to an expected 50% photoreaction. Interestingly, despite not meeting Schmidt's criteria, the non-planar linkers also exhibited photoreaction at slower rates. Furthermore, alongside UV-induced photoreaction, these compounds displayed intriguing and vigorous mechanical motion reminiscent of a photosalient effect, characterized by rolling, cracking, jumping, and fragmentation. In contrast, compound **6** demonstrated complete photoreaction due to both coordinated linkers adopting planar configurations. Additionally, these crystals exhibited a peeling effect under UV irradiation, akin to the natural peeling of tree bark due to aging. These findings highlight the potential of Zn(II)-based coordination compounds as promising candidates for developing metal-based photo actuators and optical switches, with biomimetic applications.

Introduction:

Plants exhibit fascinating responses to external stimuli, showcasing a range of mechanical motions such as bending, seed pod explosion, leaf folding, bark peeling, to name a few. These responses are vital for optimizing essential processes like photosynthesis, regeneration, and predator evasion.[1-3] Specifically, small violet flowers, known as cleistogamous flowers resemble capsules and self-pollinate through mechanical motion. During this process, the seeds from these flowers gets ejected ballistically upon dehydration.[3-4] Inspired by nature's ingenuity, researchers are developing 'actuation materials' that mimic this ability to convert light, heat, or electric fields into mechanical energy.[1, 5-6] These actuation materials inspired by nature effectively convert external stimuli, particularly light, into mechanical energy, offering tunability, remote action, intensity control, and non-invasiveness, among other advantages.[7-10]

Solid-state [2+2] photo cycloaddition reactions of olefins are particularly intriguing due to their *regio*- and *stereo*-selectivity, challenging to achieve with conventional solution methods.[11-15] These reactions offer diverse possibilities for photochemical responses within organic crystals, metal-organic compounds and polymers. Coordination compounds are known to show more structural control due to the coordination geometry of metal ions and better control on packing behavior.[16] When olefins within coordination compounds align parallelly and meet Schmidt's criteria, they engage in [2+2] cycloaddition reactions, yielding cyclobutane.[17] In recent studies it has proven that these structural transformations induce internal stress accumulation, potentially resulting in various mechanical motions such as bending, rolling, curling, splitting, breaking, and jumping in crystals also known as photosalient effect.[5, 7, 10, 18] Designing these materials is very important for the design of next generation materials and devices with significant mechanical property.[19]

The properties of materials are intricately linked to both molecular structure and crystal packing patterns. When materials exhibit similar crystal structures and packing patterns despite differences in building block compositions, they are termed isostructural.[20-22] Isostructural crystals have a high degree of structural similarity, playing a significant role in the synthesis and application of solid solutions. Several researchers have pursued the synthesis of isostructural materials for various applications. These materials also offer a promising avenue for finely tuning molecular assembly and physical and chemical properties.[23-25] However, designing and synthesizing isostructural materials is challenging, as it requires selecting molecules that occupy the same volume in the solid state despite diverse sizes, intrinsic shapes, and complex weak intermolecular interactions inherent in organic molecules.[26-27] Even slight alterations in molecular structure can significantly influence molecular packing and, consequently, material properties.[28-30]

It is known that the benzene and thiophene moieties form isostructural compounds.[31] Hence, utilization of this concepts to the metal complexes is a promising avenue for the design of photosalient materials. Herein, we report the synthesis of six photo-reactive Zn(II) halide metal complexes employing the photoreactive organic linkers 4spy, 3tpy, and 2tpy, with the molecular formulae $[ZnCl_2(4spy)_2]$, (**1**); $[ZnCl_2(3tpy)_2]$, (**2**); $[ZnCl_2(2tpy)_2]$, (**3**); $[ZnBr_2(4spy)_2]$, (**4**); $[ZnBr_2(3tpy)_2]$, (**5**); $[ZnBr_2(2tpy)_2]$, (**6**). Among these, compounds **1**, **2**, **3**, **4**, and **5** are isostructural to each other, except for compound **6**. Compound **4** has been previously reported by us.[32] All these compounds showed interesting photosalient effect.

Results and discussion

2.1. Structural Description

Brown-reddish single crystals of [$ZnCl_2(4spy)_2$], **1** have been obtained within a week by slow evaporation method in 1:2 molar ratio of $ZnCl_2$ and 4spy using DMF as crystallization solvent. These crystals were washed with methanol and dried at room temperature. The structure of this compound has been characterized through single-crystal XRD analysis which confirms that this compound is crystallized in the monoclinic $P2_1/n$ space group with Z = 4. The asymmetric unit consists of one Zn(II) atom, two chloride ions, and two 4spy ligands. The Zn(II) atom is coordinated tetrahedrally by two chloride anions and two N atoms of 4spy ligands as shown in Figure 1a. Of these, one ligand is planar while the other remains non-planar with a dihedral angle between the pyridyl ring plane and benzene ring plane is ca. 55.0° (see Figure S3a and Table S2 in supporting information, SI).

The head-to-tail (HT) alignment of the planar 4spy ligands with the neighboring 4spy linker allows [2+2] cycloaddition reaction with the centroids of the olefin units of 4spy ligands separated by 3.70 Å, within Schmidt's criteria. While the non-planar ligands didn't satisfy Schmidt's criteria, since the centroid of 4spy linkers from the neighboring molecules are separated by 5.28 Å as shown in Figure 1b. Since only one of the two 4spy linkers coordinated to Zn(II) satisfies Schmidt's criteria, compound **1** is expected to show only 50% photoreaction (Figure 1b).The phase purity of the compound has been established through PXRD studies (see Figure S1a in SI).

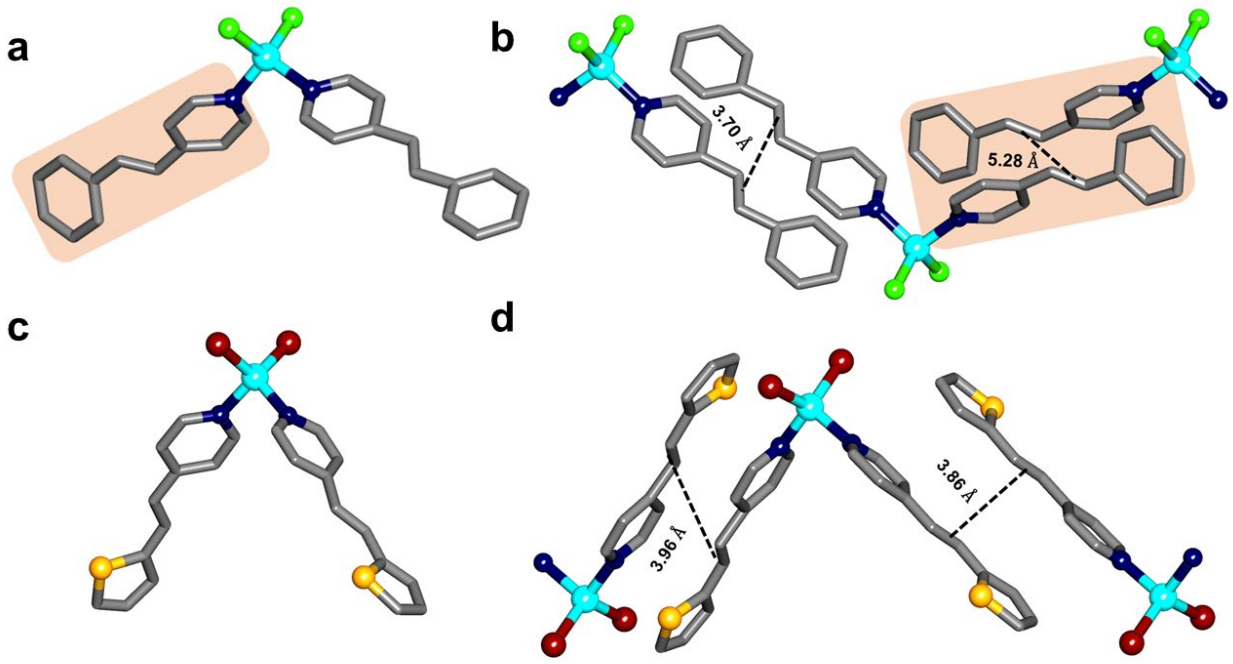

Figure 1. Illustration of crystal structures of **1** & **6** (a) Tetrahedral coordination geometry of the Zn(II) atom in **1**. Hydrogens are not shown for clarity (b) Head-to-tail alignment of planar and non-planar 4spy in **1**. (c) Tetrahedral coordination geometry of the Zn(II) atom in **6.** (d) Head-to-tail alignment of both planar 2tpy in **6**. Hydrogens are not shown for clarity.

Block shaped yellow brown single crystals of compounds **2-5** ($[ZnCl_2(3tpy)_2]$ (**2**), $[ZnCl_2(2tpy)_2]$ (**3**), $[ZnBr_2(4spy)_2]$(**4**), $[ZnBr_2(3tpy)_2]$(**5**)) were obtained using the similar reaction as **1**. The synthesis involved utilizing either $ZnCl_2$ or $ZnBr_2$ metal salts in conjunction with the photoreactive linkers 4spy, 3tpy, and 2tpy, maintaining a 1:2 molar ratio. As expected, both the chloride and bromide ions have shown similar packing as well as the phenyl and thiophene which have shown to have occupied same/similar space and resulted in the formation of isostructural compounds. All these compounds are crystallized in the monoclinic $P2_1/n$ space group, with a Z value of 4. The Zn(II) is present in tetrahedral coordination geometry which is coordinated with a planar

photoreactive linker of 4-vinylpyridine derivatives along with another non-planar linker (Figure S2). The planar linkers are aligned with the same linker from the neighboring molecule in a head-to-tail (HT) manner. The centroids of the olefins are separated by 3.33 Å, 3.70 Å, 3.72 Å, and 3.83 Å in the case of **2-5** respectively (Figure S2 in SI). Meanwhile the angle between the planes of the non-planar 4-vinylpyridine derivatives are calculated as 58.6°, 56.1°, 53.5° and 54.7° for **2-5** respectively (Figure S3 and Table S2 in SI). Further details regarding the isostructural nature of these compounds are listed in the later part of this article.

Brown-reddish single crystals of $[ZnBr_2(2tpy)_2]$ (**6**) have been obtained through slow evaporation of DMF solution of $ZnBr_2$ and 2tpy linker in 1:2 molar ratio. The structure of this compound has been characterized through single-crystal XRD analysis which confirms that this compound is crystallized in the monoclinic $P2_1/c$ space group with Z = 4. The asymmetric unit consists of one Zn(II) atom, two bromide ions and two 2tpy ligands. Although the Zn(II) atom is present in tetrahedral coordination geometry bonded by two bromide and two pyridyl linkers, (Figure 1c), both the 2tpy ligands are planar unlike the compounds **1-5**. Further, these planar 2tpy ligands in the neighboring molecules are related by the crystallographic center of inversion and are well aligned in a head-to-tail (HT) manner with the distance between the centroids of olefine is 3.86 Å and 3.96 Å (Figure 1d). The phase purity of the compound has been established through PXRD studies (see Figure S1f, in SI). Thermogravimetric analysis (TGA) revealed that **1-6** are thermally stable up to ~200 ˚C (see Figure S17 and S18 in SI).

2.2. Photoreactivity

As discussed earlier, by careful examination of the structural packing of compounds **1-5**, it is expected to observe 50% photoreaction in these compounds. This is mainly due to the alignment

of only one of the two linkers coordinated to the Zn(II) metal centers aligned in a face-to-face and head-to-tail manner, conducive to the formation of the photoproduct. This is supported by previous reports with the photoreaction of same compound, **4** indicating that only one of the two linkers undergoes photoreaction, resulting in the formation of the dimer complex.[32]

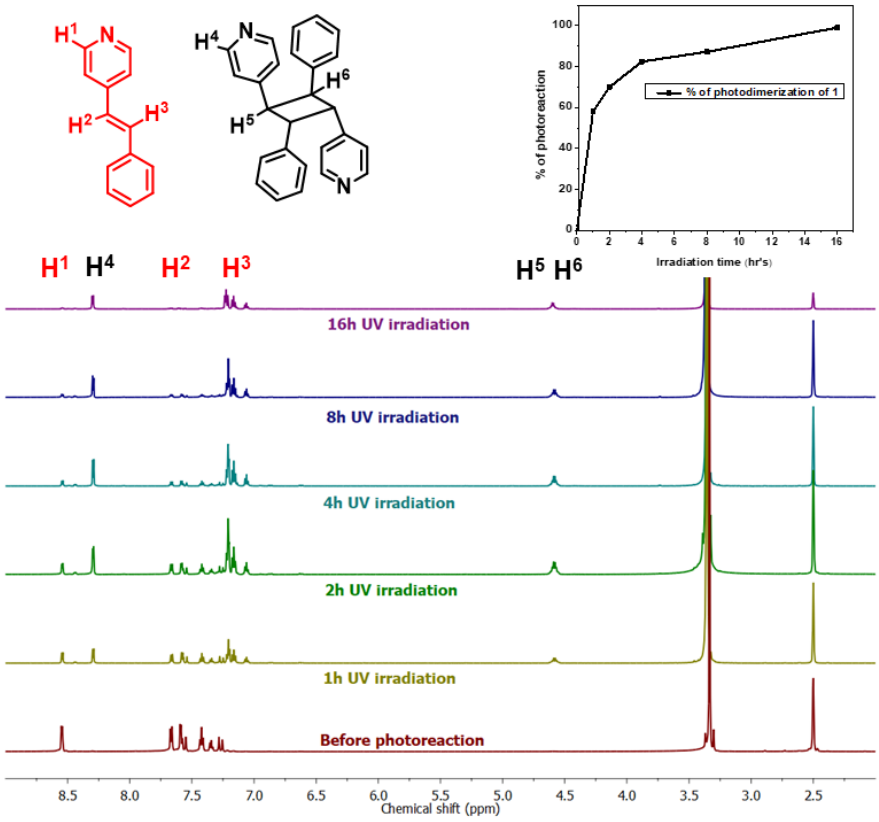

Figure 2. Time dependent ^{1}H NMR plot and time dimerization plot of **1**.

To confirm this photoreactivity these compounds were studied by analyzing the ^{1}H NMR spectrum after exposure to UV light at different time intervals using a LUZCHEM photoreactor (Figure 2). The formation of the photoproduct was confirmed by the pyridyl protons shifting from 8.5 to 8.3 ppm and the decrease in intensity of the olefin protons at 7.6 ppm and 7.2 ppm, respectively. NMR peaks at 4.5 ppm corresponding to cyclobutane began to emerge

simultaneously, confirming the photoreactive nature of the complex. According to the structural analysis and Schmidt's criteria only 50% photoreactivity is possible but the time-dimerization plot indicating almost 100% conversion in 16 h is observed (Figure 2). This may be due to molecular movements during the photoreaction under UV light and bringing the molecules, followed by the non-planar linkers close to each other and undergoing of photoreaction as per Kaupp's hypothesis, which focuses on the molecular movement within crystals.[33-35]

To understand the total possible photoreaction, the compounds are irradiated at regular intervals of time and the percentage of photoreaction is estimated and plotted against each other (see Figure 3 Figure S10-S13). Meanwhile, compound **2-5** have shown photoreaction of approximately 80, 55, 98 and 76 percentages respectively. Even further irradiation of the sample, no significant improvement in photoreactivity of these compounds has been observed.

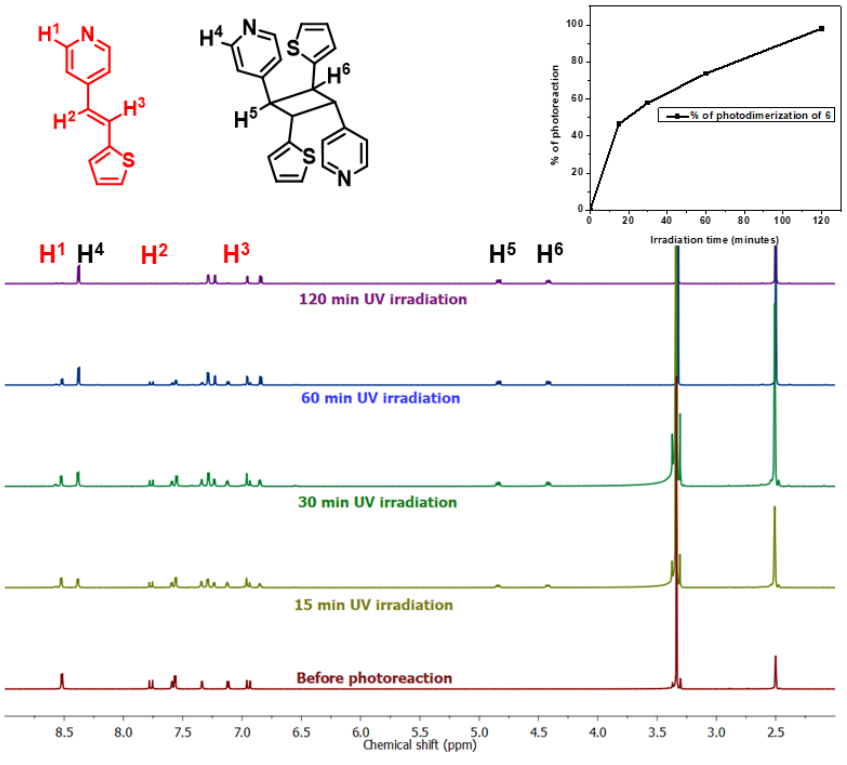

Figure 3. Time dependent ^{1}H NMR plot and time dimerization plot of **6**.

As mentioned above, this increase in photoreactivity of the samples might be explained through the movement of molecules in the solid-state during the UV-irradiation and photoreaction of the other molecules. During this movement, the non-planar linkers would come close and reorganize and undergo the photoreaction, similar to our previous report.[32] Meanwhile, the photoreactivity of compound **6** have been studied similar to other compounds. Since both the linkers are planar, aligned properly and follow Schmidt's topochemical criteria, these compounds have shown quantitative photoreaction within 120 mins, significantly faster than the other five compounds. Efforts have been made to obtain the solid-state structure of photoproduct after UV irradiation using single-crystal X-ray diffraction through both the single crystal-to-single crystal manner and recrystallization of the photo-product. Unfortunately, despite several months of effort, high-quality single crystals capable of diffracting under single-crystal XRD were not obtained. However, the photo-product structure of **4** has been previously reported by us,[21] indicating that all these compounds likely yield similar products.

2.3. Photomechanical motions

During the photoreaction under UV light, all the compounds from **1**-**5** have shown violent motion. Similar light driven mechanical motions are reported for past few years by both our groups along with various other researchers, also known as photosalient effect.[5, 18, 36-37] This behavior is significantly helpful in the conversion of light energy into mechanical motion. To study such photosalient behavior, various single crystals of each compound have been exposed to UV light under microscope which is connected to the high-resolution high-speed camera. Studies with high-speed camera have shown that all the crystals are shown different kind of motions, including breaking of the crystals, rolling, exploding, bending and jumping under UV irradiation.

The photomechanical motion of single crystals was monitored using UV light (390 nm) through an optical microscope equipped with a high-speed camera and in some cases normal cameras. When single crystals of compound **1** were exposed to UV light, they broke into small pieces and immediately jumped apart with a rolling motion. This photo-induced actuation occurred within a very short duration as shown in Figure 4 (see Videos in supporting files). Similarly, single crystals of compounds **2**, **3**, **4**, and **5** displayed breaking, rolling, and jumping apart, as shown in the videos. The mechanical jumping of these crystals is clearly evidenced by SEM as shown in Figure S14.

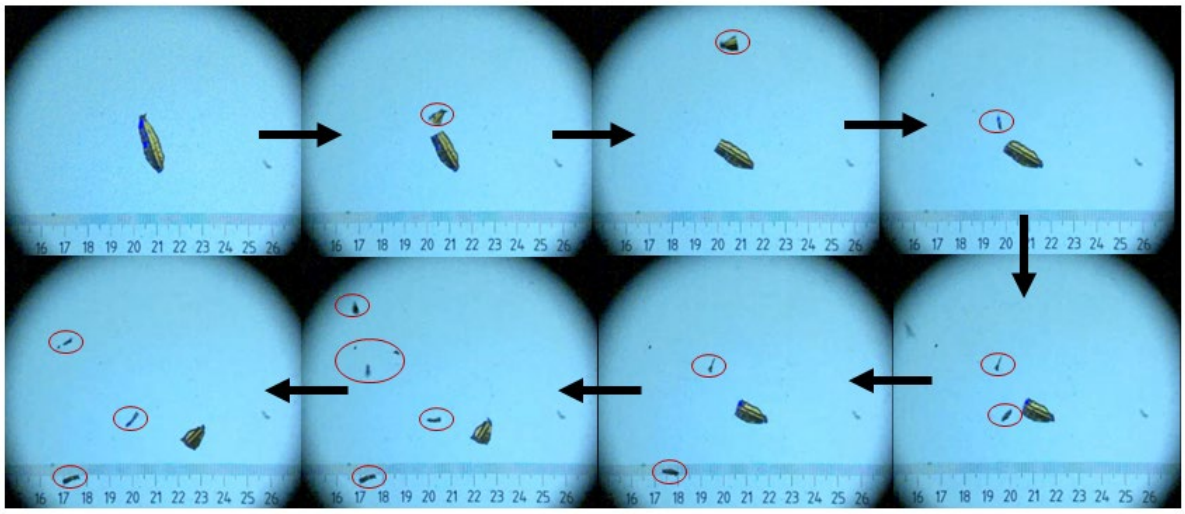

Figure 4. Optical images depicting the mechanical motion of compound **1** under UV light exposure were captured using a high-speed camera connected to a stereo microscope.

Possibly due to differences in molecular arrangement and packing behavior compared to other compounds, compound **6** exhibits a notable variation in mechanical properties during photoreaction. This compound demonstrates a rare phenomenon known as the peeling effect, which is uncommon in the realm of photo responsive materials and single crystals.[38-39] Under UV irradiation, the photoreaction initiates from the edges of the single crystals and progresses towards

the center, resulting in significant peeling of layers, as depicted in Figure 5. This mechanism bears resemblance to the natural process of tree bark peeling over time. Analogously, the outer layers of tree trunks peel off with age, mirroring the behavior observed in our single crystals due to photoreaction. Scanning electron microscope images further confirm this peeling phenomenon, as illustrated in Figure S14f.

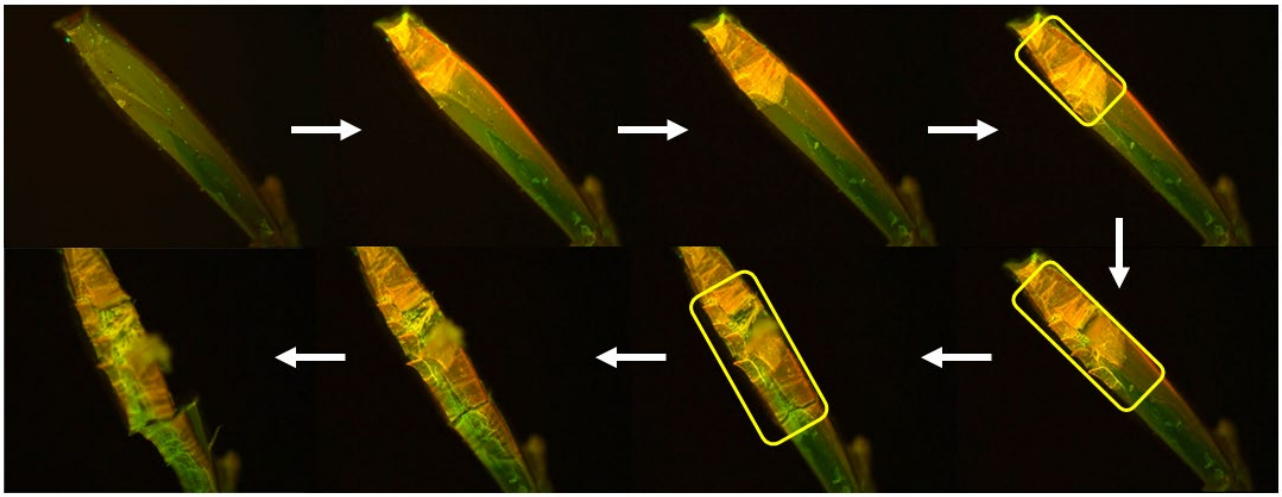

Figure 5. The series of images of $[ZnBr_2(2tpy)_2]$ under photoirradiation with time (excited at 390 nm) (left to right) under fluorescence microscope. The white arrow shows the reactivity of the compound which is unidirectional. The reactivity of the crystals in the layer manner which could be observed by rolling of the layers followed by the formation of cracks in the crystal which is highlighted in yellow.

2.4. Isostructural analysis

As designed, replacing the phenyl group with thiophene was expected to produce isostructural compounds. To confirm this, we systematically compared single crystal structures and cell parameters. Preliminary studies revealed that compounds **1-5** crystallized in the $P2_1/n$ space group

with very similar unit cell parameters, while compound **6** crystallized in $P2_1/c$ with different unit cell parameters (Table S1). Similarly, unit cell similarity index (denoted as π) has been calculated by comparing the cell parameters of the materials using the following formula,[21, 24, 40-41]

$$\pi = [(a + b + c) / (a' + b' + c')] - 1$$

Here, a, b, c, a', b', and c' represent the orthogonalized lattice parameters of the unit cells of the respective materials. Based on the calculated π values against the lattice parameter of each compound, it is evident that compounds **1**-**5** have π values close to zero, indicating similarity in their cell parameters, as shown in Table S3. This observation suggests that these compounds are likely to exhibit isostructurality, implying similar crystal structures. Upon comparing the π values for each material, as presented in Table S3, it becomes evident that all values are close to zero, confirming the materials' isostructural nature. Consequently, we can infer that all complexes share very similar crystal structures. Notably, compound **6** also exhibits similar π values, despite its distinct structural packing behavior. This finding warrants further analysis of the isostructural nature within this context.

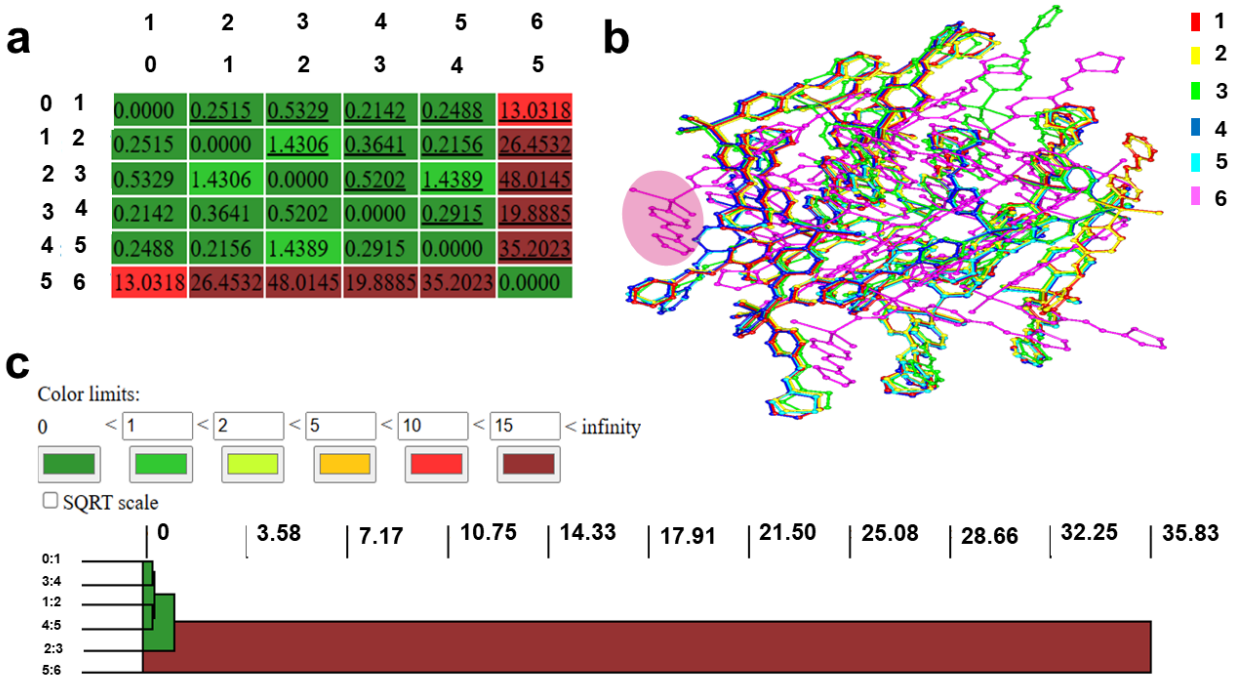

Figure 6. (a) Similarity matrix of **1-6** (b) Overlay of **1-6,** showing that except **6** all are well overlayed on each other. (c) Dendrogram calculated from the similarity matrix showing the packing similarity of **1-5** and **6** not similar.

To accurately quantify the isostructurality, we further utilized CrystalCMP software to analyze the similarity in molecular packing of these compounds.[42-44] The CMP dendrogram and similarity matrix, revealed lower PS_{ab} values (less than 1.5) for **1-5**, and reported. On the other hand, **6** has a very high PS_{ab} value (more than 10) as shown in Figure 6a. Therefore, the relatively low values of PS_{ab} obtained from the calculation results indicate that the packing of **1-5** are similar. The stacking of the crystal structure shown in Figure 6b demonstrated that complexes **1-5** are well overlapped with each other, indicating that they are isostructural whereas **6** does not overlap with any of the other crystal structures. From the comparison, it clearly shows that only **1-5** are isostructural to each other. To support this, we calculated the angle between the planes of the pyridyl group and benzene/thiophene as shown in Table S2 and Figure S3. This revealed that the

Zn(II) in **6** is attached with two planar linkers, whereas in the remaining complexes, all Zn(II) are attached with one planar and one non-planar linker. Due to this, **6** is not overlapped with other complexes. Hence it is clear that **1-5** are isostructural to each other.

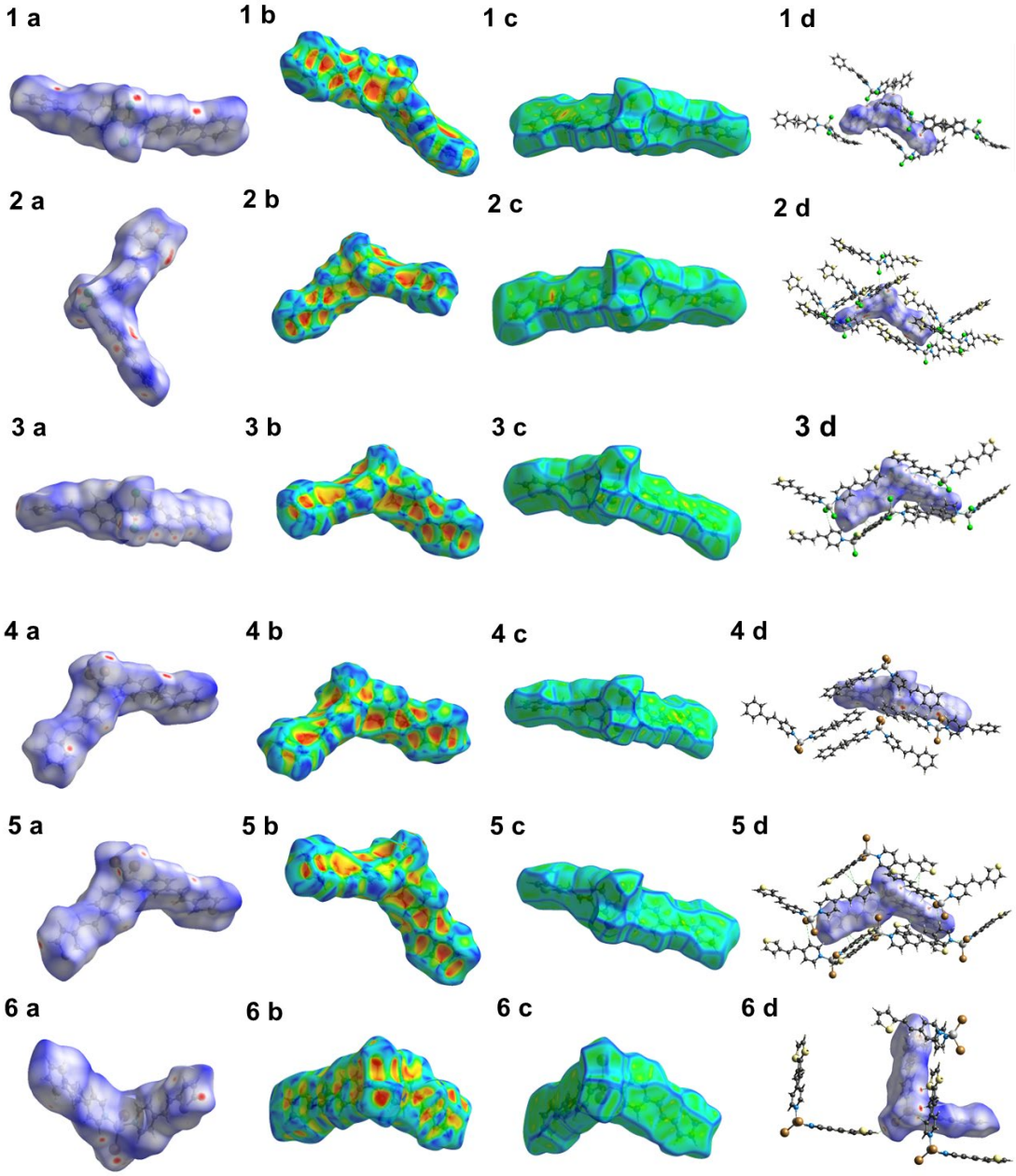

Figure 7. Hirshfeld surface plotted (a) d_{norm} (b) Shape index (c) Curvedness (d) of **1-6** complexes (d) Viewing of short contacts in the Hirshfeld surface plotted over d_{norm} of **1-6** complexes.

2.5. Hirshfeld surface analysis

To better understand the intermolecular interactions responsible for molecular packing in crystals, Hirshfeld analysis was carried out. To generate the molecular surface analysis required for this analysis, Crystal Explorer software was employed.[19, 21, 45-47] The resulting Hirshfeld surface mapped over d_{norm} is highlighted in the Figure 7. The normalized contact distance, d_{norm}, is defined as follows.

$$d_{norm} = [(d_i - r_i^{vdw})/r_i^{vdw}] + [(d_e - r_e^{vdw})/r_e^{vdw}]$$

Here, d_i and d_e represent the distances from each point on the surface to the nearest nuclei internal and external to the surface, respectively. The value of d_{norm} can be negative or positive, depending on whether the intermolecular contacts are shorter or longer than the van der Waals radii, respectively. The bright red regions on the surface indicate interactions that are shorter than the van der Waals radii, with a negative d_{norm} value. The blue regions on the surface are from interactions that are longer than the van der Waals radii, with a positive d_{norm} value. The white regions are from neutral contacts with a zero d_{norm} value.

The 2D fingerprint plot of the compounds, shown in the Figure S16, was generated in the d_{norm} range of 0.6 to 2.8 Å. This plot shows the percentage contribution of each contact to the total Hirshfeld surface area. The highlighted blue area and the length of spikes are due to the strong contacts, such as H···H, C···H, Br/Cl-··H, etc., present in the crystal packing of all complexes. The percentage contribution of these intermolecular interactions is quantified in the Figure 8, with H···H interaction contributing the largest percentage in all the complexes. Besides, C···C, C···H,

Br/Cl···H, and S···H, N···H are other important interactions, but the percentage of their contribution varies with the specific crystal structure.

It is worth noting that, in all studied crystal structures, compound **6** has Br···Br interactions compared to the other crystal structures but the percentage of this is very minimum. In addition, this compound lacks Br···C interaction as shown in Figure 8. From this, it is clear that the crystal packing of **6** is different from that of the rest due to different intermolecular interactions.

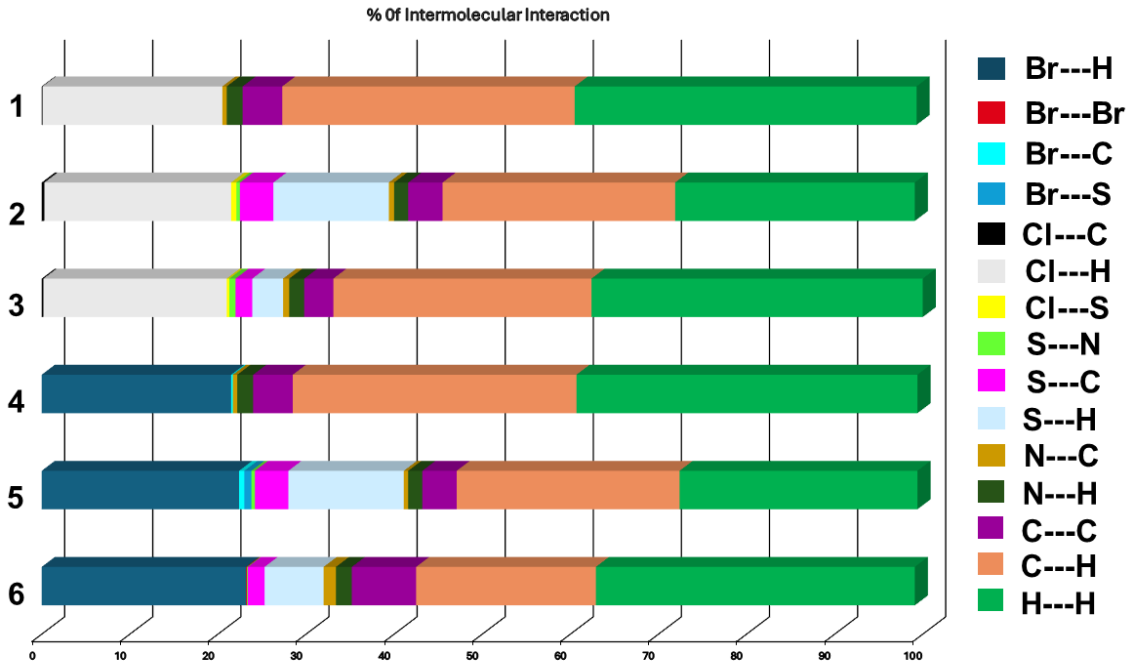

Figure 8. Relative contribution of intermolecular interaction to the Hirshfeld surface in **1-6**.

When Hirshfeld surface (HS) is mapped over the surface index of the complexes, a bow-tie pattern of red (concave) and blue (convex) triangles can be seen in Figure 7. This triangular-shaped region on the HS plotted over the shape index indicates the presence of C···C interactions, which means π···π stacking interactions are present in the crystal packing. The higher the

percentage of C···C interactions, the stronger the π···π stacking is. In all studied crystal structures **6** has a higher percentage of C···C interactions, which is almost double compared to other crystal structures as shown in Figure 8. This is also supported by the flat regions on HS mapped with curvedness as shown in Figure 7, for **6** two ligands in the asymmetric unit are covered by the flat regions whereas for the rest only one photo ligand in the asymmetric unit is covered by the flat region.

2.6. Photoluminescence

Optical studies were conducted to investigate the absorption and luminescence properties of six compounds. Solid-state UV-Vis absorption spectroscopy revealed that all the compounds exhibited photo absorption below ~390 nm (Figure S19). The emission properties were studied by exciting the compounds at 350 nm. Interestingly, although all the compounds (**1-5**) have the same packing behavior, there is a systematic shift in emission properties based on the linker (e.g., 4spy, 3tpy, and 2tpy) (Table S4). However, no significant role of halides has been observed. Furthermore, fluorescence lifetime measurements indicated an increase in the average lifetime based on the linker (Table S5 and S6), with no significant impact from halides. These findings suggest that isostructural analysis is intriguing, as it allows for the modification of emission properties without altering the molecular packing and the use of phenyl-thiophene exchange.

Additionally, the emission properties of these compounds were studied both before and after the photoreaction. These studies confirmed a significant red shift in emissions after the photoreaction, along with a decrease in emission intensity (as shown in Figure S20 in the SI). This shift may be attributed to the disruption in the delocalization of the photoreactive linker during the photoreaction, altering the charge transfer between the metal and the linker.[48]

Conclusions

In conclusion, our study has presented six photoreactive Zn(II) metal complexes using 4-vinylpyridine derivatives, coupled with chloride or bromide co-linkers. Through structural characterization, we confirmed the isostructural nature of compounds **1-5**, with slight variations observed in compound **6**. Compounds **1-5** demonstrated partial photoreaction due to coordination of two linkers, one with planar geometry and other with non-planar geometry. While compound **6** exhibited complete photoreaction owing to both coordinated linkers adopting planar configurations. Despite deviations from Schmidt's criteria, non-planar linkers also displayed slower photoreaction rates. Compounds **1**-**5** exhibited dynamic mechanical motion akin to rolling, cracking, jumping, and fragmentation, under UV light. Whereas compound **6** has shown peeling effect similar to tree bark along with quantitative photoreaction, might be due to difference packing behavior and non-covalent interactions. Overall, our findings highlighted the potential of these Zn(II) coordination compounds as promising candidates for the development of metal-based photoactuators and optical switches, offering new insights into biomimetic mechanical motion and photosalient phenomena. Further exploration of their properties and applications could contribute to advancements in materials science and crystal engineering.

ASSOCIATED CONTENT

Supporting Information. Materials and methods, synthesis of compounds, X-ray data, PXRD, ^{1}H-NMR spectra, Solid-State UV-Visible spectra, photoluminescence spectra, TGA, SEM, TRPL, CrystalCMP, and Hirshfeld details and videos with mechanical motions.

AUTHOR INFORMATION

Corresponding Authors

Raghavender Medishetty* - Department of Chemistry, Indian Institute of Technology Bhilai, Kutelabhata, Durg, 491001, Chhattisgarh, India. raghavender@iitbhilai.ac.in; ragha.chem@gmail.com

Mohammad Hedayetullah Mir* - Department of Chemistry, Aliah University, New Town, Kolkata 700160, India. chmmir@gmail.com

Authors

Uma Kurakula‡ - Department of Chemistry, Indian Institute of Technology Bhilai, Kutelabhata, Durg, 491001, Chhattisgarh, India.

Akansha Ekka‡ - Department of Chemistry, Indian Institute of Technology Bhilai, Kutelabhata, Durg, 491001, Chhattisgarh, India.

Basudeb Dutta - Department of Chemistry, Aliah University, New Town, Kolkata 700160, India.

Nathan R. Halcovitch - Chemistry Department, Lancaster University, Faraday Building, Lancaster University, Lancaster, LA1 4YB, UK.

‡ These authors contributed equally.

Author Contributions

The manuscript was written through contributions of all authors. All authors have given approval to the final version of the manuscript.

‡These authors contributed equally.

Funding Sources

R.M. acknowledges IBITF (Grant No. IBITF/PRAYAS/Note/2023-24/0009) and M.H.M. acknowledges SERB, India (Grant No. CRG/2022/001842, dated 19/12/2022) for financial support.

ACKNOWLEDGMENT

We thank Dr. Veera Reddy, IISER Trivandrum, for his continuous support with NMR measurements. We also thank Mrs. Anshumika Mishra, Siksha 'O' Anusandhan University, Bhubaneswar and Ms. Pyarija S. Lal, NISER Bhubaneswar for their support. R.M. acknowledges IBITF (Grant No. IBITF/PRAYAS/Note/2023-24/0009) and M.H.M. acknowledges SERB, India (Grant No. CRG/2022/001842, dated 19/12/2022) for financial support. The authors acknowledge Central Instrumentation Facility (CIF), IIT Bhilai, for providing the PXRD and SEM facilities. U.K. thanks UGC for the fellowship.

REFERENCES

1. Naumov, P.; Chizhik, S.; Panda, M. K.; Nath, N. K.; Boldyreva, E., Mechanically Responsive Molecular Crystals. *Chem. Rev.* **2015,** *115* (22), 12440-12490.

2. Lancia, F.; Ryabchun, A.; Katsonis, N., Life-like motion driven by artificial molecular machines. *Nature Reviews Chemistry* **2019,** *3* (9), 536-551.

3. Little, R. J.; Leiper, G., Capsule Dehiscence in Viola betonicifolia Sm. (Violaceae). *Austrobaileya* **2012,** *8* (4), 624-633.

4. Cullen, J., *Handbook of North European Garden Plants: With Keys to Families and Genera*. Cambridge University Press: 2001.

5. Rath, B. B.; Vittal, J. J., Photoreactive Crystals Exhibiting [2 + 2] Photocycloaddition Reaction and Dynamic Effects. *Acc. Chem. Res.* **2022,** *55* (10), 1445-1455.

6. Naumov, P.; Karothu, D. P.; Ahmed, E.; Catalano, L.; Commins, P.; Mahmoud Halabi, J.; Al-Handawi, M. B.; Li, L., The Rise of the Dynamic Crystals. *J. Am. Chem. Soc.* **2020,** *142* (31), 13256-13272.

7. Rath, B. B.; Vittal, J. J., Dynamic effects in crystalline coordination polymers. *CrystEngComm.* **2021,** *23*, 5738-5752.

8. Zhu, L.; Tong, F.; Al-Kaysi, R. O.; Bardeen, C. J., Photomechanical Effects in Photochromic Crystals. In *Photomechanical Materials, Composites, and Systems*, John Wiley & Sons, Ltd: 2017; pp 233-274.

9. Hu, Y.; Li, Z.; Lan, T.; Chen, W., Photoactuators for Direct Optical-to-Mechanical Energy Conversion: From Nanocomponent Assembly to Macroscopic Deformation. *Adv. Mater.* **2016,** *28* (47), 10548–10556.

10. Zhou, B.; Yan, D., Recent advances of dynamic molecular crystals with light-triggered macro-movements. *Appl. Phys. Rev.* **2021,** *8* (4), 041310.

11. Vittal, J. J., Supramolecular structural transformations involving coordination polymers in the solid state. *Coord. Chem. Rev.* **2007,** *251* (13-14 SPEC. ISS.), 1781-1795.

12. Medishetty, R.; Park, I.-H.; Lee, S. S.; Vittal, J. J., Solid-state polymerisation via [2+2] cycloaddition reaction involving coordination polymers. *Chem. Commun.* **2016,** *52* (21), 3989-4001.

13. Kole, G. K.; Mir, M. H., Isolation of elusive cyclobutane ligands via a template-assisted photochemical [2 + 2] cycloaddition reaction and their utility in engineering crystalline solids. *CrystEngComm.* **2022,** *24*, 3993-4007.

14. Biradha, K.; Santra, R., Crystal engineering of topochemical solid state reactions. *Chem. Soc. Rev.* **2013,** *42* (3), 950-967.

15. Georgiev, I. G.; MacGillivray, L. R., Metal-mediated reactivity in the organic solid state: from self-assembled complexes to metal-organic frameworks. *Chem. Soc. Rev.* **2007,** *36* (8), 1239-1248.

16. Zhang, Q.; Wang, Y.; Braunstein, P.; Lang, J.-P., Construction of olefinic coordination polymer single crystal platforms: precise organic synthesis, in situ exploration of reaction mechanisms and beyond. *Chem. Soc. Rev.* **2024,** *53* (10), 5227-5263.

17. Schmidt, G. M. J., Photodimerization in the solid state. *Pure & Appl. Chem.* **1971,** *27*, 647-678.

18. Khan, S.; Akhtaruzzaman; Medishetty, R.; Ekka, A.; Mir, M. H., Mechanical Motion in Crystals Triggered by Solid State Photochemical [2+2] Cycloaddition Reaction. *Chem. Asian J.* **2021,** *16* (19), 2806-2816.

19. McGehee, K.; Saito, K.; Kwaria, D.; Minamikawa, H.; Norikane, Y., Releasing a bound molecular spring with light: a visible light-triggered photosalient effect tied to polymorphism. *Phys. Chem. Chem. Phys.* **2024,** *26* (8), 6834-6843.

20. Kálmán, A.; Párkányi, L.; Argay, G., Classification of the isostructurality of organic molecules in the crystalline state. *Acta Crystallogr. Sect. B.* **1993,** *49* (6), 1039-1049.

21. Wojnarska, J.; Gryl, M.; Seidler, T.; Stadnicka, K. M., Effect of Substituent Exchange on Optical Anisotropy in Multicomponent Isostructural Materials Containing Sulfathiazole and 2-Aminopyridine Derivatives. *Cryst. Growth. Des.* **2020,** *20* (10), 6535-6544.

22. Cinčić, D.; Friščić, T.; Jones, W., A cocrystallisation-based strategy to construct isostructural solids. *New J. Chem.* **2008,** *32* (10), 1776-1781.

23. Suresh, K.; Khandavilli, U. B. R.; Gunnam, A.; Nangia, A., Polymorphism, isostructurality and physicochemical properties of glibenclamide salts. *CrystEngComm.* **2017,** *19* (6), 918-929.

24. Medishetty, R.; Ekka, A.; Mulijanto, C. E.; Tandiana, R.; Vittal, J. J., Isostructurality in amino molecular salts of two dicarboxylic acids driven by noncovalent synthons. *CrystEngComm.* **2022,** *24* (36), 6330-6337.

25. Burrows, A. D., Mixed-component metal–organic frameworks (MC-MOFs): enhancing functionality through solid solution formation and surface modifications. *CrystEngComm.* **2011,** *13* (11), 3623-3642.

26. Dey, A.; Desiraju, G. R., Supramolecular equivalence of ethynyl, chloro, bromo and iodo groups. A comparison of the crystal structures of some 4-phenoxyanilines. *CrystEngComm.* **2004,** *6* (104), 642-646.

27. Giangreco, I.; Cole, J. C.; Thomas, E., Mining the Cambridge Structural Database for Matched Molecular Crystal Structures: A Systematic Exploration of Isostructurality. *Cryst. Growth. Des.* **2017,** *17* (6), 3192-3203.

28. Bhunia, S.; Sahoo, D.; Dutta, B.; Maity, S.; Manik, N. B.; Sinha, C., Correlation in Structural Architecture toward Fabrication of Schottky Device with a Series of Pyrazine Appended Coordination Polymers. *Inorg. Chem.* **2023,** *62* (51), 20948-20960.

29. Bhunia, S.; Sahoo, D.; Maity, S.; Dutta, B.; Bera, S.; Manik, N. B.; Sinha, C., Aminoisophthalate Bridged Cd(II)-2D Coordination Polymer: Structure Description, Selective Detection of Pd2+ in Aqueous Medium, and Fabrication of Schottky Diode. *Inorg. Chem.* **2023,** *62* (30), 11976-11989.

30. Dutta, B.; Halder, S., Fabrication of Schottky Barrier Diodes Utilizing Schiff Base Compounds and Metal Complexes with Schiff Base Ligands. *ChemistrySelect* **2023,** *8* (24), e202301586.

31. Thallapally, P. K.; Chakraborty, K.; Carrell, H. L.; Kotha, S.; Desiraju, G. R., Shape and size effects in the crystal structures of complexes of 1,3,5-trinitrobenzene with some trigonal donors: The benzene-thiophene exchange rule. *Tetrahedron* **2000,** *56* (36), 6721-6728.

32. Medishetty, R.; Yap, T. T. S.; Koh, L. L.; Vittal, J. J., Thermally reversible single-crystal to single-crystal transformation of mononuclear to dinuclear Zn(II) complexes by [2+2] cycloaddition reaction. *Chem. Commun.* **2013,** *49* (83), 9567-9569.

33. Kaupp, G., Photodimerization of Cinnamic Acid in the Solid State: New Insights on Application of Atomic Force Microscopy. *Angew. Chem. Int. Ed. Engl.* **1992,** *31* (5), 592-595.

34. Kaupp, G., Organic Solid-State Reactions with 100% Yield. In *Organic Solid State Reactions*, Toda, F., Ed. Springer Berlin Heidelberg: Berlin, Heidelberg, 2005; pp 95-183.

35. Nagarathinam, M.; Vittal, J. J., A Rational Approach to Crosslinking of Coordination Polymers Using the Photochemical [2+2] Cycloaddition Reaction. *Macromol. Rapid. Commun.* **2006,** *27* (14), 1091-1099.

36. Ping, X.; Pan, J.; Peng, X.; Yao, C.; Li, T.; Feng, H.; Qian, Z., Recent advances in photoresponsive fluorescent materials based on [2+2] photocycloaddition reactions. *J. Mater. Chem. C,* **2023,** *11* (23), 7510-7525.

37. Morimoto, K.; Kitagawa, D.; Bardeen, C. J.; Kobatake, S., Cooperative Photochemical Reaction Kinetics in Organic Molecular Crystals. *Chem. Eur. J.* **2023,** *29* (14), e202203291.

38. Nakagawa, Y.; Morimoto, M.; Yokojima, S.; Nakamura, S.; Uchida, K., Efficient Surface Peeling, a Photoinduced Result of Photochromic Diarylethene Crystal by Multistep Light Irradiation. *Cryst. Growth. Des.* **2023,** *23* (3), 1581-1591.

39. Nakagawa, Y.; Morimoto, M.; Yasuda, N.; Hyodo, K.; Yokojima, S.; Nakamura, S.; Uchida, K., Photosalient Effect of Diarylethene Crystals of Thiazoyl and Thienyl Derivatives. *Chem. Eur. J.* **2019,** *25* (33), 7874-7880.

40. Fabian, L.; Kalman, A., Volumetric measure of isostructurality. *Acta Crystallogr. Sect. B.* **1999,** *55* (6), 1099-1108.

41. Jha, K. K.; Dutta, S.; Kumar, V.; Munshi, P., Isostructural polymorphs: qualitative insights from energy frameworks. *CrystEngComm.* **2016,** *18* (43), 8497-8505.

42. Li, Z.; Zhou, J.; Zhang, K.; Zhang, Y.; Wu, S.; Gong, J., Playing with Isostructurality from Binary Cocrystals to Ternary Cocrystal Solvates of Quercetin: Tuning Colors of Pigment. *Cryst. Growth. Des.* **2022,** *22* (9), 5322-5334.

43. Hughes, D. S.; Bingham, A. L.; Hursthouse, M. B.; Threlfall, T. L.; Bond, A. D., The extensive solid-form landscape of sulfathiazole: geometrical similarity and interaction energies. *CrystEngComm.* **2022,** *24* (3), 609-619.

44. Rohlíček, J.; Skořepová, E.; Babor, M.; Čejka, J., CrystalCMP: an easy-to-use tool for fast comparison of molecular packing. *J. Appl. Crystallogr.* **2016,** *49* (6), 2172-2183.

45. Ashfaq, M.; Munawar, K. S.; Tahir, M. N.; Dege, N.; Yaman, M.; Muhammad, S.; Alarfaji, S. S.; Kargar, H.; Arshad, M. U., Synthesis, Crystal Structure, Hirshfeld Surface Analysis, and Computational Study of a Novel Organic Salt Obtained from Benzylamine and an Acidic Component. *ACS Omega* **2021,** *6* (34), 22357-22366.

46. Ranjan, S.; Devarapalli, R.; Kundu, S.; Saha, S.; Deolka, S.; Vangala, V. R.; Reddy, C. M., Isomorphism: `molecular similarity to crystal structure similarity' in multicomponent forms of analgesic drugs tolfenamic and mefenamic acid. *IUCrJ* **2020,** *7* (2), 173-183.

47. Spackman, P. R.; Turner, M. J.; McKinnon, J. J.; Wolff, S. K.; Grimwood, D. J.; Jayatilaka, D.; Spackman, M. A., CrystalExplorer: a program for Hirshfeld surface analysis, visualization and quantitative analysis of molecular crystals. *J. Appl. Crystallogr.* **2021,** *54* (3), 1006-1011.

48. Ekka, A.; Kurakula, U.; Choudhury, A.; Mishra, A.; Faye, A.; Halcovitch, N. R.; Medishetty, R., Light-driven flagella-like motion of coordination compound single crystals. *Chem. Commun.* **2023,** *59* (29), 4384-4387.

For Table of Content use only:

Photoreactive Zn(II) Coordination Compounds: Exploring Biomimetic Mechanical Motion and Photosalient Behavior

Uma Kurakula,[a,‡] Akansha Ekka,[a,‡] Basudeb Dutta,[c] Mohammad Hedayetullah Mir,[c] Nathan Halcovitch,[b] and Raghavender Medishetty*[a]*

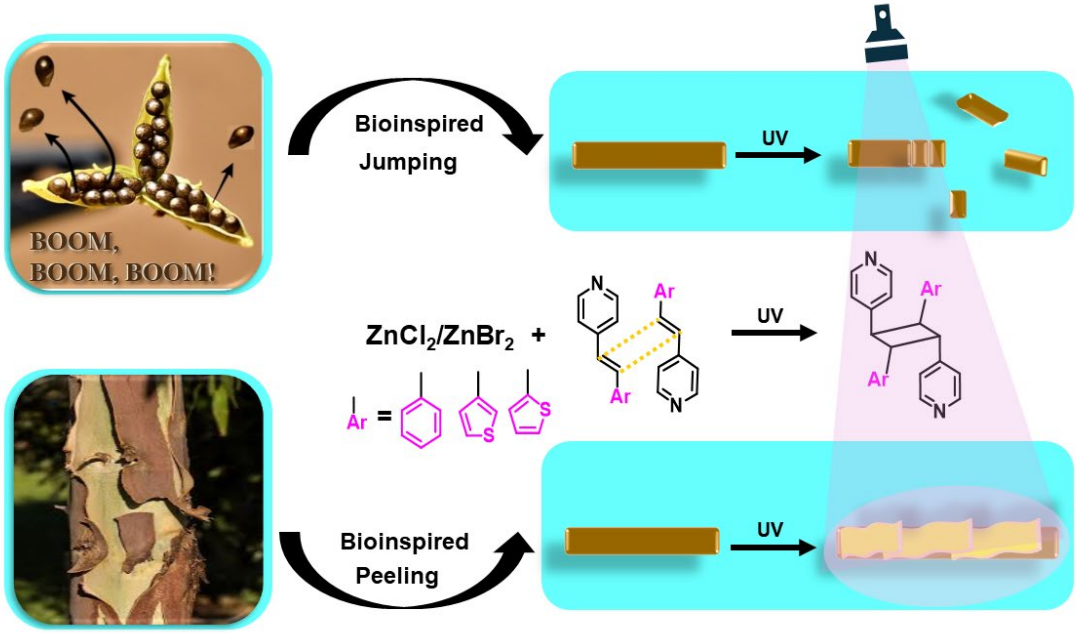

Six photoreactive Zn(II)-based coordination compounds exhibiting significant mechanical motion, including explosive behavior, under UV light. These compounds demonstrate isostructural characteristics and vigorous mechanical responses such as rolling, cracking, and fragmentation, highlighting their potential in developing metal-based photo actuators and optical switches for advanced biomimetic applications.